DOI 10.5012/bkcs.2009.30.12.3113

Organic-Free Au-Pd Alloys on Germanium Substrate *via* Spontaneous Galvanic Displacement Reaction

Kang Yeol Lee, Sang Woo Han,†,* and Hee Cheul Choi*

*Department of Chemistry and Division of Advanced Materials Science, Pohang University of Science and Technology (POSTECH), Pohang 790-784, Korea. *E-mail: choihc@postech.edu*
*†Department of Chemistry and KI for the NanoCentury, KAIST, Daejeon 305-701, Korea. *E-mail: sangwoohan@kaist.ac.kr*
Received September 1, 2009, Accepted October 20, 2009.

Key Words: Organic-free, Galvanic displacement, Au-Pd Alloys, Co-deposition

The unique electrical and optical properties of semiconductor and metal nanocrystals have been attracted for their potential applications in nanoelectronics, optoelectronics, catalysis, and biomedical imaging/therapeutics.[1-7] Since these properties are dramatically affected by the sizes and geometrical shapes of nanocrystals, various chemical synthetic strategies have been developed to precisely control the aforementioned factors. A representative approach to synthesize semiconductor or metal nanocrystals employs the reaction of precursors in solution phase at elevated temperature in the presence of organic stabilizing agents which prohibit severe aggregation of the produced nanocrystals[1,3] Although this traditional synthetic method has successfully produced various nanocrystals having very narrow size distributions, the presence of organic molecules on their surfaces frequently causes problems as a significant barrier, for example, in electron and photon transports.

Recently, a facile chemical approach enabling spontaneous formations of metal nanocrystals on solid substrates in the absence of organic stabilizing agent has been developed.[8-13] The galvanic displacement, a mechanism-based nomenclature for the spontaneous metal nanocrystal formation, involves direct electron transfer from metal or semiconductor substrates (electron donors) to metallic precursor cations (electron acceptors) at room temperature according to their relative electrochemical redox potentials. A representative example of metal nanocrystals synthesized by the galvanic displacement is Au nanoparticles on germanium (Ge) surface.[8] In this case, the electrons spontaneously donated by Ge fully reduce Au^{3-} ions into Au nanocrystals when both species are simply brought into contacts in aqueous solution. To take the best advantage of its simplicity, the galvanic displacement process has been mostly applied to synthesize monometallic noble metal nanocrystals such as Au, Ag, Pd, Pt, and *etc.*[8-13] on Ge or other semiconductors such as GaAs, InP substrate, of which cations generally have significantly large positive standard reduction potential values. On the contrary, there is not much report about the formation of composite alloys which are of great interest from scientific and technological perspectives owing to their composition-dependent optical, catalytic, electronic, and magnetic properties.[14]

Herein we introduce the spontaneous formation of Au-Pd alloys *via* galvanic displacement process, which is the first demonstration of organic-free bimetallic alloy crystals to the best of our knowledge. The galvanic displacement derived direct formation of Au-Pd bimetallic nanostructures on Ge substrate is confirmed by using scanning electron microscopy (SEM), transmission electron microscopy (TEM), energy-dispersive X-ray spectroscopy (EDS), X-ray diffraction (XRD), and surface-enhanced Raman scattering (SERS). The organic-free Au-Pd alloys are anticipated to exhibit high catalytic activities on the conventionally applied reactions such as synthesis of hydrogen peroxide,[15] hydrodesulfuriztion of thiophene derivatives, hydrogenation of aromatics,[16,17] and oxidation of alcohols to aldehydes.[18]

Experimental

Chemicals. $HAuCl_4$ (99.9+%) and Na_2PdCl_4 (99.998%) were used as purchased from Aldrich. Other chemicals, unless specified, were reagent grade, and deinoized water (R > 18.0 MΩ) was used when preparing aqueous solutions. Ge wafers (Ga-doped p-type Ge(100), resistivity: 0.005 - 0.1 Ω·cm) were used as a substrate.

Preparation of Au-Pd alloy films. In a typical synthesis of Au-Pd bimetallic thin films, 100 μL of premixed aqueous solution of $HAuCl_4$ (concentration of stock solution: 5 mM) and Na_2PdCl_4 (concentration of stock solution: 5 mM) was added into 900 μL of deionized water to make the final 1 mM solution. To this solution, a piece of Ge wafer substrate precleaned with isopropanol and dried under N_2 flow was immersed. After 12 hr, the Ge substrate containing Au-Pd bimetallic alloy films was thoroughly rinsed with deionized water to remove unreacted precursors, then dried under ambient conditions.

Characterization of Au-Pd alloy thin films. TEM images were obtained using a Philips CM 200 transmission electron microscope operating at 200 kV. High-resolution TEM (HR-TEM) and scanning TEM (STEM) images were acquired using a JEOL JEM-2100F (200 kV) transmission electron microscope equipped with a field emission gun and an ultra-high-resolution observation system. This instrument includes a scanning image device to operate as STEM from TEM in a serial manner. It also possesses several atom level probes connected to Oxford INCA X-ray energy dispersive spectrometer and Gatan 2D digital-parallel acquisition software. The electron probe size and dwell time used in the STEM-EDS mapping experiments were 0.1 nm and 0.2 ms per pixel, respectively.

The SEM and EDS data of the samples were taken with a field emission scanning electron microscope (FESEM, Phillips Model XL30 S FEG). The XRD patterns were obtained using a Bruker AXS D8 DISCOVER diffractometer with a Cu K_α (1.5406 Å) radiation. For SERS measurements, Ge substrates containing Au, Pd, and Au-Pd bimetallic films were soaked in 1 mM 1,4-phenylenediisocyanide (1,4-PDI) in ethanol solution overnight, then washed with ethanol and dried under ambient conditions. Raman spectra were obtained using a Jobin Yvon/HORIBA LabRAM spectrometer with 632.8 nm line of an air-cooled He/Ne laser as an excitation source.

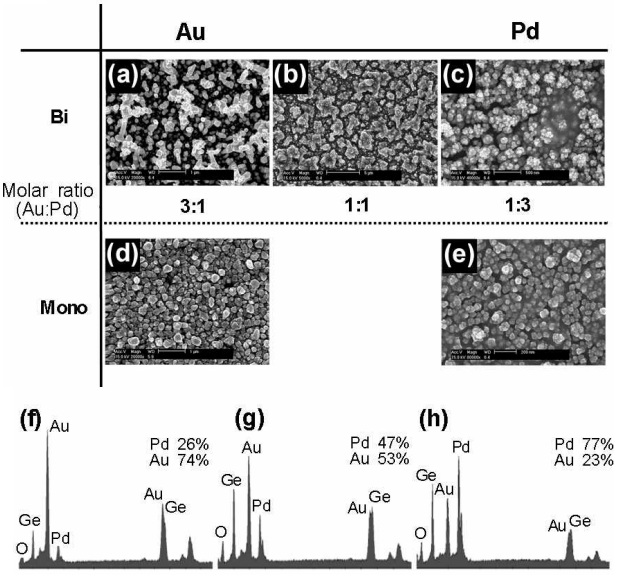

Figure 1. SEM images of bimetallic (a) Au-Pd (3:1), (b) Au-Pd (1:1), (c) Au-Pd (1:3), and monometallic (d) Au, (e) Pd nanocrystal films formed *via* spontaneous galvanic displacement process on Ge substrates. EDS spectra of (f) Au-Pd (3:1), (g) Au-Pd (1:1), and (h) Au-Pd (1:3) films on Ge substrates.

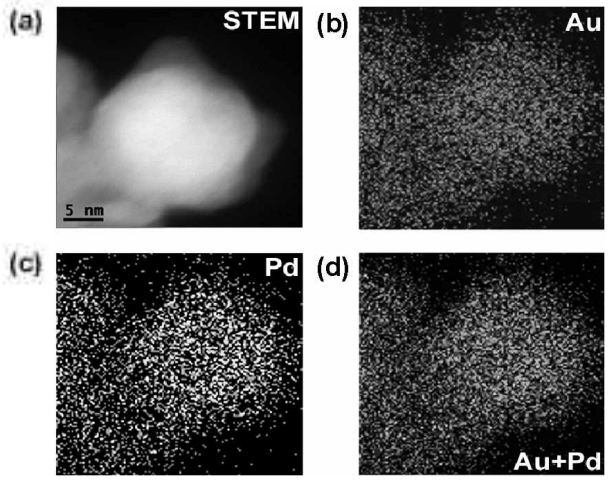

Figure 2. (a) High-magnification STEM image of Au-Pd (1:1) bimetallic particle, (b-d) STEM-EDS mapping images of (a): (b) Au mapping image, (c) Pd mapping image, and (d) overlapped image of (b) and (c).

Results and Discussion

When a piece of Ge wafer was soaked into the solution of $HAuCl_4/Na_2PdCl_4$ mixture, a thin film of Au-Pd bimetallic nanocrystals was readily formed on the Ge surface within 1 hr. As shown in Figure 1, the resulting films are composed of numerous nanocrystallites while their morphologies are slightly but obviously varied according to the ratios of Au to Pd. As the content of a specific component in the mixed precursor solution is increased, the morphology of the product resembles that of its pure component. For example, the Au-Pd films prepared from the $HAuCl_4/Na_2PdCl_4$ mixture solution having 3:1 molar ratio (Au-Pd (3:1) in Figure 1a) shows individual nanocrystals with an average diameter of approximately 174 nm, which is similar to that of pure Au film of which average diameter is slightly lager (approximately 266 nm, Figure 1d). Similarly, the Au-Pd film prepared from the $HAuCl_4/Na_2PdCl_4$ mixture solution having 1:3 molar ratio (Au-Pd (1:3) in Figure 1c) displays similar morphology to that of pure Pd film (Figure 1e) as satellite-type nanocrystal aggregations are found from both of them (for clarity, see the larger size SEM images (Figure S1) in Supplementary Electronic Material). Meanwhile, the morphology of Au-Pd alloy prepared from Au-Pd (1:1) solution shows a unique morphology that is dissimilar to either pure Au or Pd (Figure 1b). Note that the pure Au and Pd nanocrystal films were prepared by soaking Ge wafers into 1 mM of $HAuCl_4$ and 1 mM of Na_2PdCl_4 aqueous solutions, respectively, at room temperature for 12 hr.

To qualitatively confirm the formation of Au-Pd bimetallic particles, we examined the chemical composition changes of the Au-Pd films by EDS attached to SEM. The results indicate that the mole fractions of Pd in Au-Pd (3:1), Au-Pd (1:1), and Au-Pd (1:3) bimetallic films are 0.26, 0.47, and 0.77, respectively (Figure 1f-h), which are closely consistent with the molar ratios in the feeding solutions. The distribution and homogeneity of each component in individual Au-Pd nanocrystallites were further characterized by STEM-EDS analyses. According to the typical STEM image of a bimetallic Au-Pd (1:1) particle (Figure 2a) and EDS mapping data (Figure 2b-d), Au and Pd atoms are uniformly distributed over the entire particle without any predominance of specific component.

The formation of Au-Pd alloys was further confirmed by systematically investigating their XRD patterns with those of films composed of Au and Pd individual nanocrystals (Figure 3a-e). Each XRD pattern exhibits two major diffraction peaks in the range of $35^\circ < 2\theta < 50^\circ$, which are originated from (111) and (200) planes of the *fcc* metallic Au and Pd structures. In the case of pure Au nanocrystal film, the 2θ values corresponding to the diffractions from Au (111) and Au (200) are 38° and 44°, respectively (Figure 3a). When Pd contents are gradually increased, these two peaks are systematically shifted to higher 2θ values, and eventually getting closer to the 2θ values of 40° and 47° corresponding to Pd (111) and Pd (200) (Figure S2). To further confirm whether such a systematic shift is indeed distinctive for the formation of Au-Pd alloy rather than individual Au and Pd nanocrystals, we examined diffraction patterns with samples prepared (1) by sequential treatment with 1.0 mM $HAuCl_4$ followed by with 1.0 mM Na_2PdCl_4

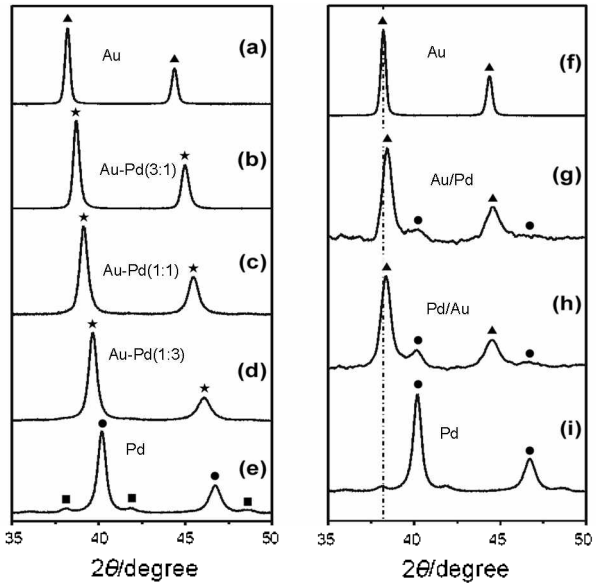

Figure 3. (a-e) XRD patterns of Au, Au-Pd and Pd nanocrystal films prepared on Ge substrates by the simultaneous galvanic displacement reaction from mixed aqueous solutions of $HAuCl_4$/ Na_2PdCl_4. (f-i) XRD patterns of Au, Au/Pd, Pd/Au, and Pd nanocrystal films. Note that Au/Pd and Pd/Au were prepared by sequential galvanic displacement reactions. (▲: Au, ●: Pd, ★: Au-Pd, ■: GeO_2).

solutions on a Ge substrate (Au/Pd, Figure 3g), and (2) by sequential treatment with 1.0 mM Na_2PdCl_4 followed by 1.0 mM $HAuCl_4$ solutions on a Ge substrate (Pd/Au, Figure 3h).[19] As shown in Figure 3g and h, four peaks in total corresponding to the peaks from individual Au (triangles) and Pd (circles) are simultaneously observed without a noticeable shift. Note that the small peaks at 38°, 42° and 49° in Figure 3e (squares) are originated from GeO_2 (JCPDS No. 04-0497).[20] The molar compositions of Au and Pd in the alloy thin films could be also estimated by the lattice parameter shifts calculated from the angular positions of the (111) diffractions according to Vegard's law.[21] The mole fractions of Pd in Au- Pd (3:1), Au-Pd (1:1), and Au-Pd (1:3) alloy thin films were estimated to be 0.26, 0.46, and 0.74, respectively, which agrees well with the aforementioned EDS results.

The successfully formed Au-Pd alloys would populate both Au and Pd on their surfaces. Such well-developed surfaces were evaluated by SERS measurements with 1,4-PDI as an adsorbate. It has been reported that isocyanides are readily adsorbed on noble metals such as Au,[22,23] Ag,[24] Pd,[23] and Pt[25] through the metal-CN bonds, of which bonding types are distinctively different depending on the kinds of metal substrates. For example, isocyanides adsorb on Au and Pd surfaces *via* pure σ interaction and σ/π synergistic interaction, respectively. Therefore, the scattering peaks at various energies due to different degrees of bonding characters can become a signature for the surface nature. The surface of Au-Pd alloys adsorbed with 1,4-PDI would exhibit scattering features originated from both Au and Pd developed on the Au-Pd alloy surfaces. Indeed, significant differences were observed in the SERS spectra upon the adsorption of 1,4-PDI on Au, Pd, and

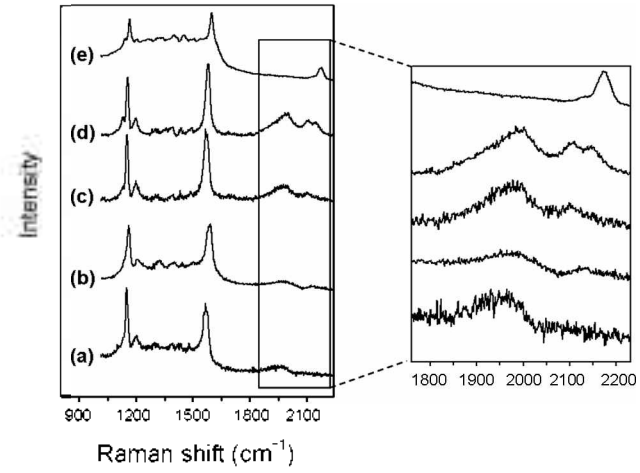

Figure 4. SERS spectra of 1,4-PDI on (a) Pd, (b) Au-Pd (1:3), (c) Au-Pd (1:1), (d) Au-Pd (3:1), and (e) Au films. All spectra were normalized with 8a mode peak at 1600 cm^{-1} for more easy comparison.

Au-Pd alloy films. While the characteristic NC stretching band appeared at 1965 cm^{-1} (strong and broad) and 2120 cm^{-1} (very weak) on pure Pd surface (Figure 4a), the corresponding peak appeared at 2170 cm^{-1} in the case of pure Au surface (Figure 4e). In contrast, the SERS spectra of 1,4-PDI on Au-Pd alloy films show peaks in two regions at around 1970 cm^{-1} and 2150 cm^{-1} which should be originated from Pd and Au, respectively (Figure 4b-d). This result indicates that the surface of Au-Pd alloy is populated with both Au and Pd, which is in a good agreement with the previous report.[26] 1,4-PDI molecules are supposed to adsorb on Au entirely at the on-top site, whereas both the on-top site and the 3-fold hollow site (open-faced trinuclear metal clusters) are occupied by 1,4-PDI molecules in the case of Pd surface.[23] When 1,4-PDI molecules bind to Au-Pd alloy particles, instead of simple mixture of Au and Pd particles, the adsorption of 1,4-PDI molecule would be more complicated due to the co-presence of preferred binding sites of which populations are significantly varied according to the population of exposed Au and Pd on the surface of Au-Pd alloy particles. Such a complicated adsorption phenomenon is an another indirect evidence for the successful formation of Au-Pd alloy particles, and indeed represented in the Raman spectra as a peak shift (red-shift toward lower frequency, Figure 4b-d) and peak split shown at near 2140 cm^{-1} (Figure 4d).

The co-deposition of two different metal ions into alloys has been widely studied for various applications, which is frequently quoted as an anomalous electrodeposition due to its lack of understanding about the mechanism.[27-30] Although the mechanism for the formation of Au-Pd alloy by the spontaneous reduction of $AuCl_4^-$ and $PdCl_4^{2-}$ ions by Ge is not clear yet, several feasible scenarios can be suggested. First, $AuCl_4^-$ ions are expected to be reduced first by Ge over $PdCl_4^{2-}$ even when they are co-present since the reduction of $AuCl_4^-$ is thermodynamically much favorable considering their standard reduction potential values ($E^\circ_{AuCl_4^-/Au}$ = +1.002 V and $E^\circ_{PdCl_4^{2-}/Pd}$ = +0.591 V *vs* standard hydrogen electrode (SHE)) as shown in Figure 6.[31] Then, Au deposits would catalyze the further re-

duction of $PdCl_4^{2-}$,[32] resulting in Au-Pd alloys. Meanwhile, the thermodynamic advantage does not always necessarily decide the sequence of reduction of metal ions coexisting in a solution. For example, in Zn-Ni alloys prepared by electrochemical co-deposition from a solution containing both Ni^{2+} and Zn^{2+} ions, Zn has been always richer than Ni in the products despite its thermodynamic disadvantage ($E^{\circ}_{Zn^{2+}/Zn} = -0.762$ V and $E^{\circ}_{Ni^{2+}/Ni} = -0.257$ V *vs* SHE).[33-35] For the similar sense, we cannot exclude another possible mechanism for the Au-Pd alloys that involves the first reduction of $PdCl_4^{2-}$ ions followed by the Au-Pd alloy formation through the spontaneous charge transfer from Pd^0 to $AuCl_4^-$ ions (E° for $Pd + AuCl_4^- \rightleftharpoons Au + PdCl_4^{2-}$ is +0.401 V).

Conclusions

The spontaneous formation of Au-Pd bimetallic films *via* galvanic displacement at room temperature was successfully demonstrated. The composition ratio of Au and Pd of the alloys are controlled by simply controlling the mole fractions of Pd to Au in the precursor mixture solution. The formation of Au-Pd alloys rather than individual Au and Pd monometallic nanocrystals was confirmed by the systematic shifts of XRD peaks of (111) and (200) planes and by the SERS intensity originated from the chemical interactions of 1,4-PDI on Au-Pd alloys. Since the Au-Pd alloys formed by the galvanic displacement are free from organic capping or structure directing molecules that may have played as a barrier for charge carrier mobility, they are expected to realize the performance improvement in various applications including nanoelectronics, catalysis, fuel cell, hydrogen sensor, and other related fields.

Acknowledgments. This study was supported by a grant of the Korea Healthcare technology R&D Project, Ministry for Health, Welfare & Family Affairs, Korea (A090062), and partly by the National Research Foundation of Korea (NRF) grant funded by MEST (2008-04306, 2007-8-1158, 2005-01325), KOSEF through EPB center (R11-2008-052-02000). H.C.C thanks the World Class University (WCU) program (R31-2008-000-10059-0). We also thank Prof. Su-Moon Park at UNIST for fruitful discussion.

Supporting Information. The SEM images of Figure S1a-e are available on request from the correspondence author.

References

1. Burda, C.; Chen, X.; Narayanan, R.; El-Sayed M. A. *Chem. Rev.* **2005**, *105*, 1025-1102.
2. Rosi, N. L.; Mirkin, C. A. *Chem. Rev.* **2005**, *105*, 1547-1562.
3. Ozin, G. A.; Arsenult, A. C. *Nanochemistry: A Chemical Approach to Nanomaterials* RSC Publishing: *Cambridge*, 2005.
4. Cheon, J.; Lee, J.-H. *Acc. Chem. Res.* **2008**, *41*, 1630-1640.
5. Dhar, S.; Reddy, E.; Shiras, A.; Pokharkar, V.; Prasad, B. *Chem. Eur. J.* **2008**, *14*, 10244-10250.
6. Liu, H.; Chen, D.; Tang, F.; Du, G.; Li, L.; Meng, X.; Liang, W.; Zhang, Y.; Teng, X.; Li, Y. *Nanotechnology* **2008**, *19*, 455101.
7. Hauck, T. S.; Jennings, T. L.; Yatsenko, T.; Kumaradsa, J. C.; Chan, W. C. W. *Adv. Mater.* **2008**, *20*, 3832-3838.
8. Porter, L. A.; Choi, H. C.; Buriak, J. M. *Nano Lett.* **2002**, *2*, 1067-1071.
9. Porter, L. A.; Ribbe, A. E.; Buriak, J. M. *Nano Lett.* **2003**, *3*, 1043-1047.
10. Aizawa, M.; Cooper, A.; Malac, M.; Buriak, J. M. *Nano Lett.* **2005**, *5*, 815-819.
11. Aizawa, M.; Buriak, J. M. *J. Am. Chem. Soc.* **2005**, *127*, 8932-8933.
12. Hormozi Nezhad, M. R.; Aizawa, M.; Porter, L. A.; Ribbe, A. E.; Buriak, J. M. *Small* **2005**, *1*, 1076-1081.
13. Sayed, S. Y.; Daly, B.; Buriak, J. M. *J. Phys. Chem. C* **2008**, *112*, 12291-12298.
14. Toshima, N.; Yonezawa, T. *New J. Chem.* **1998**, *22*, 1179-1201.
15. Edwards, J. K.; Hutchings, G. J. *Angew. Chem. Int. Ed.* **2008**, *47*, 9192-9198.
16. Venezia, A. M.; La Parola, V.; Deganello, G.; Pawelec, B.; Fierro, J. L. G. *J. Catal.* **2003**, *215*, 317-325.
17. Pawelec, B.; Cano-Serrano, E.; Campos-Martin, J. M.; Navaro, R. M.; Thomas, S.; Fierro, J. L. G. *Appl. Catal. A* **2004**, *275*, 127-139.
18. Enache, D. I.; Edwards, J. K.; Landon, P.; Solsona-Espriu, B.; Carley, A. F.; Herzing, A. A.; Watanabe, M.; Kiely, C. J.; Knight, D. W.; Hutchings, G. J. *Science* **2006**, *311*, 362-365.
19. 1.0 mL of aqueous solutions of 1.0 mM $HAuCl_4$ and 1.0 mM Na_2PdCl_4, were prepared. A piece of Ge wafer was immersed into the aqueous solution of 1.0 mM $HAuCl_4$. After 15 min, the germanium wafer was rinsed with deionized water, and immersed again into the aqueous solution of 1.0 mM Na_2PdCl_4 for another 15 min (Au/Pd). The resulting Ge substrate was thoroughly rinsed with deionized water to remove unreacted precursors, and then dried under ambient conditions. The opposite sequential reaction was applied to prepare Pd/Au sample.
20. Kim, H. W.; Shim, S. H.; Lee, J. W. *Appl. Sur. Sci.* **2007**, *243*, 7207-7210.
21. Damle, C.; Kumar, A.; Sastry, M. *J. Phys. Chem. B* **2002**, *106*, 297-302.
22. Kim, N. H.; Kim, K. *J. Phys. Chem. B* **2006**, *110*, 1837-1842.
23. Swanson, S. A.; McClain, R.; Lovejoy, K. S.; Alamdari, N. B.; Hamilton, J. S.; Scott, J. C. *Langmuir* **2005**, *21*, 5034-5039.
24. Han, H. S.; Han, S. W.; Joo, S. W.; Kim, K. *Langmuir* **1999**, *15*, 6868-6874.
25. Garrell, R. L. *Anal. Chem.* **1989**, *61*, 401A-411A.
26. Lee, Y. W.; Kim, N. H.; Lee, K. Y.; Kwon, K.; Kim, M.; Han, S. W. *J. Phys. Chem. C* **2008**, *112*, 6717-6722.
27. Chang, B.-Y.; Park, S. M. *J. Electrochem. Soc.* **2004**, *151*, C786-C788.
28. Hovestad, A.; Janssen, L. J. J. *J. App. Electrochem.* **1995**, *25*, 519-527.
29. Chi, Q. J.; Dong, S. J. *Anal. Chim. Acta* **1995**, *310*, 429-436.
30. Zech, N.; Podlaha, E. J.; Landolt, D. *J. Electrochem. Soc.* **1999**, *146*, 2886-2891.
31. *CRC Handbook of Chemistry and Physics*, 84th ed.; Lide, D. R., Ed.; CRC Press: Boca Raton, FL, 2004.
32. Nutt, M. O.; Heck, K. N.; Alvarez, P.; Wong, M. S. *Applied Catalysis B: Environmental* **2006**, *69*, 115-125.
33. Miranda, F. J. F.; Barcia, O. E.; Mattos, O. R.; Wiart, R. *J. Electrochem. Soc.* **1997**, *144*, 3441-3449.
34. Nichol, M. J.; Philip, H. I. *J. Electroanal. Chem.* **1976**, *70*, 233-237.
35. Chassaing, E.; Wiart, R. *Electrochim. Acta* **1992**, *37*, 545-553.